

Ground states of the doped four-leg t - J ladder

Steven R. White

Department of Physics and Astronomy, University of California, Irvine, California 92697

D. J. Scalapino

Department of Physics, University of California, Santa Barbara, California 93106

(Received 2 April 1997)

Using density-matrix renormalization-group techniques, we have studied the ground states of the four-leg t - J ladder doped near half-filling. Depending upon J/t and the hole doping x , three characteristic types of ground states are found: (1) a state containing $d_{x^2-y^2}$ pairs, (2) a striped charge-density wave (CDW) domain-wall state, and (3) a phase-separated regime. The CDW domain walls consist of fluctuating hole pairs and this state has significant $d_{x^2-y^2}$ pair field correlations. [S0163-1829(97)51222-7]

The observation of spin gaps^{1,2} in the two-leg SrCu_2O_3 and four-leg $\text{La}_2\text{Cu}_2\text{O}_5$ ladder compounds and the recent report of superconductivity in a hole doped $(\text{La,Sr,Ca})_{14}\text{Cu}_{24}\text{O}_{41}$ compound containing CuO_2 chains and two-leg Cu_2O_3 ladders³ has brought renewed interest in the properties of even-leg metal-oxide ladders. Here, using density-matrix renormalization group (DMRG) techniques,⁴ we study the t - J model of a four-leg ladder for a range of J/t values and dopings near half-filling. We have observed three types of ground states: (1) a state containing a dilute gas of $d_{x^2-y^2}$ -like pairs; (2) a striped charge-density wave (CDW) domain-wall state, where each domain wall consists of four holes; and (3) a phase-separated regime. Here we show examples of each type of state and discuss the interplay between CDW and pairing correlations appearing in these states.

The Hamiltonian for the t - J model is

$$\mathcal{H} = -t \sum_{\langle ij \rangle, s} P_G (c_{i,s}^\dagger c_{j,s} + c_{j,s}^\dagger c_{i,s}) P_G + J \sum_{\langle ij \rangle} (\vec{S}_i \cdot \vec{S}_j - \frac{1}{4} n_i n_j), \quad (1)$$

where $c_{i,s}^\dagger$ and $\vec{S}_i = c_{i,\alpha}^\dagger \vec{\sigma}_{\alpha\beta} c_{i,\beta}$ are electron creation and spin operators respectively, n_i is the occupation number operator, P_G is the Gutzwiller projection operator which excludes configurations with doubly occupied sites, and $\langle ij \rangle$ denotes nearest neighbor sites. Here we report results for ladders with open boundary conditions for hole dopings of $0 \leq x \leq 0.25$ and various J/t values. Our calculations for the four-leg ladders were carried out using a DMRG method in which transformation matrices were stored and used to construct the initial state for each superblock diagonalization.⁵ Of order 10^3 states were kept per block, and the final transformation matrices were used to calculate the ground state expectation values of the desired operators at the end of the calculation.

The types of ground states which we have found are illustrated in Fig. 1. The results shown in Fig. 1 are for a 20×4 lattice with from 8 to 16 holes. These figures represent

the most probable configuration of holes in the system, obtained by maximizing the ground-state expectation value of a hole projection operator

$$P(l_1, l_2, \dots) = \prod_{i=1} p(l_i), \quad (2)$$

where $p(l) = (1 - n_{l\uparrow})(1 - n_{l\downarrow})$ is the hole projection operator for the l th lattice site. The results shown in Fig. 1 were obtained by maximizing $\langle P(l_1) \rangle$ over l_1 , then maximizing $\langle P(l_1, l_2) \rangle$ over l_2 with fixed l_1 , etc., until all the holes have been located. Although this procedure is not guaranteed to give the maximum of $\langle P(l_1, l_2, \dots) \rangle$ over all $\{l_i\}$, we have not observed any cases in which it appears to fail. The positions of the holes are shown as the solid circles in Fig. 1.

These pictures of most-likely hole configurations are representative of the three types of ground states which we have found for dopings $0 < x < 0.25$, with $0.25 < J/t < 3$. Figure

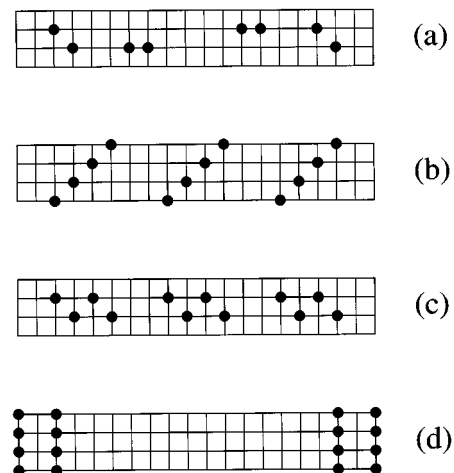


FIG. 1. Maximum-likelihood hole configurations obtained by maximizing the expectation value of $P(l_1, l_2, \dots)$, Eq. (2), for various ground states of the doped four-leg t - J ladder. (a) A gas of pairs with $J/t=0.35$ and a filling of $x=0.1$. (b) “Diagonal” (1,1) domain walls with $J/t=0.5$ and $x=0.15$. (c) “Zigzag” domain walls with $J/t=0.25$ and $x=0.15$. (d) Phase separation with $J/t=2.0$ and $x=0.2$.

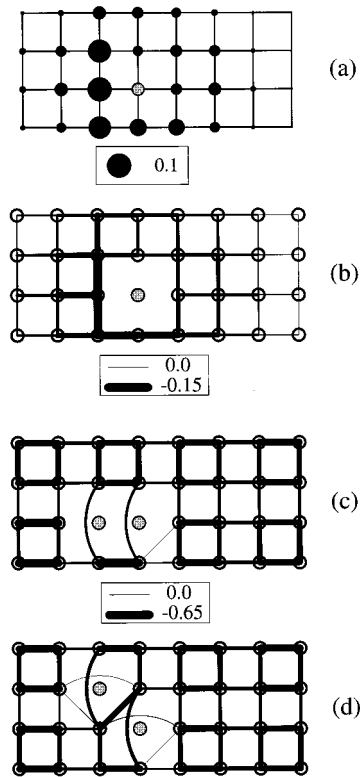


FIG. 2. A pair in the pair-gas state, with $J/t=0.35$ and $x=0.1$. We show the second pair from the left in Fig. 1(a). (a) The diameter of the black dots shows the probability of finding the second member of a hole pair at that site when the first hole has been projected out at the gray shaded position. All of the holes in other pairs have also been projected out. (b) The width of the lines indicates the magnitude of the hopping kinetic energy of one member of a pair when the other is projected out at the shaded site. (c) The expectation value of $\vec{S}_i \cdot \vec{S}_j$ between various sites when the holes are nearest neighbors and (d) when they are next-nearest neighbors.

1(a) shows a gas of pairs, which occurs at low doping levels for a wide range of J/t , in this case $x=0.1$, $J/t=0.35$. At higher doping levels, four-hole clusters (or two-pair clusters) form, giving what we will call the domain-wall states shown in Figs. 1(b) and 1(c). Figure 1(b) shows a diagonal domain-wall state for $J/t=0.5$, $x=0.15$, where the most probable hole configuration has four holes along a diagonal. For smaller values of J/t , the most probable hole configuration consists of a zigzag pattern along the two center chains, as shown in Fig. 1(c) for $x=0.15$, $J/t=0.25$. Although it appears that there are two different types of domain walls shown in Figs. 1(b) and 1(c), as we discuss below, fluctuations in the walls lead us to consider these to be the same type of state. Phase separation, as shown in Fig. 1(d), where the holes have all moved to either end of the ladder, occurs for J/t greater than about 1.5–1.9, in this case $J/t=2$. For $J/t \sim 3$, the holes become closely packed at the ends of the ladder.⁶

In order to obtain a clearer picture of the nature of these pair-gas and domain-wall states, we have examined various local correlations. Figure 2(a) shows the probability of various hole configurations near the most likely configuration for the system shown in Fig. 1(a), focusing on the second pair

from the left. The diameter of the dots is proportional to the probability of the last hole being on that site, when all the other hole positions are fixed. In this case the last hole is the left-hand hole of the second pair in Fig. 1(a). Although the maximum point shown in Fig. 1(a) has this pair as nearest neighbors, the probability of the last hole being on either the site above or below the maximum point is nearly as large. The results are consistent with Lanczos calculations for two holes on a periodic $\sqrt{26} \times \sqrt{26}$ lattice, in which for $J/t=0.35$ the holes are about 20% more likely to be found across a diagonal than on near-neighbor sites.^{7,8} Figure 2(b) shows the expectation value of the kinetic energy on each bond when the location of all but one of the holes [the same hole as in Fig. 2(a)] has been specified by the projection operator.

The expectation value of $\vec{S}_i \cdot \vec{S}_j$ near the paired holes in the two most likely configurations of Fig. 2(a) is shown in Figs. 2(c) and 2(d). In these plots, the width of the lines is proportional to the bond strength $-\langle \vec{S}_i \cdot \vec{S}_j \rangle$. In addition to showing the nearest-neighbor correlations, we show next-nearest-neighbor correlations when both sites are adjacent to the same hole, but only when these correlations are antiferromagnetic, $\langle \vec{S}_i \cdot \vec{S}_j \rangle < 0$. Antiferromagnetic correlations coupling next-nearest-neighbor sites across dynamic holes is an almost universal feature of the doped t - J model,⁹ and presumably other doped antiferromagnets. These frustrating correlations develop in order to minimize the kinetic energy.⁹ The strong diagonal singlet correlation crossing the hole pair in Fig. 2(d) is a striking example of this effect. The kinetic energy term strongly favors a singlet bond connecting these sites since for four of the eight hops available to the holes in this configuration, this bond becomes a nearest-neighbor exchange bond. This diagonal singlet is characteristic of a $d_{x^2-y^2}$ pair.⁹

A closer view of the domain walls in Figs. 1(b) and 1(c) is shown in Fig. 3. The probability of finding at a given site the fourth hole making up a diagonal domain wall is shown in Fig. 3(a). This shows that while the (1,1) direction is favored, the domain wall is fluctuating strongly. At larger values of J/t (e.g., $J/t \sim 1$) the (0,1) direction becomes favored. The expectation value of the exchange field $\vec{S}_i \cdot \vec{S}_j$ for this wall is plotted in Fig. 3(b). A number of its features are similar to those of the hole pair in Fig. 2(d), such as the presence of diagonal singlets. However, in a diagonal domain wall the undoped spin background is broken into two unconnected parts by the wall, eliminating the frustration. The kinetic energy of a wall is not as low as that of two isolated pairs, making the walls unstable at low hole densities for moderate values of J/t .

The kinetic energy favors hole configurations that avoid the edge sites and near-neighbor sites, while the exchange energy favors these, leading to competition. An example of this competition is seen in the most probable location of a pair in the pair-gas state. For $J/t=0.5$, pairs are found primarily on outer chains in order to form undoped two-leg ladder structures.^{9,10} For $J/t=0.35$, the tendency of the holes to avoid the edge sites is slightly stronger, and pairs are more likely to be found on the two middle chains, as shown in Figs. 1(a) and 2(a). For smaller values of J/t , this tendency of the holes to avoid the edge sites affects the structure of a

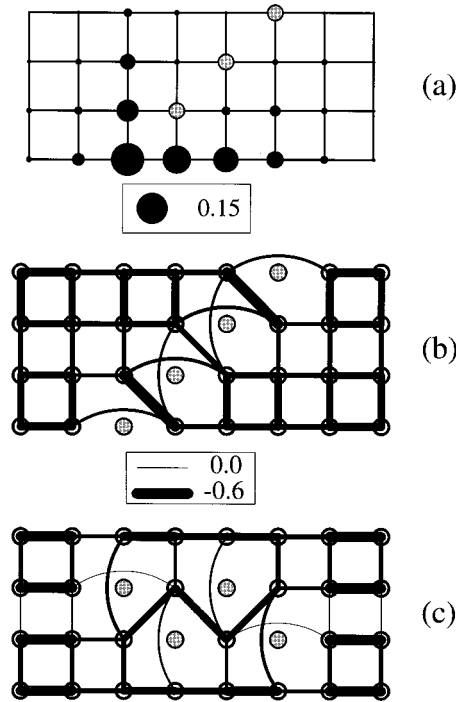


FIG. 3. A section of a 20×4 lattice showing a domain wall, with $J/t=0.5$ and $x=0.15$, as in Fig. 1(b). (a) The probability of finding the fourth hole when the others have been projected out, and (b) the expectation value of $\vec{S}_i \cdot \vec{S}_j$ when all holes have been projected out in their most likely configuration. (c) Same as (b), but for the system shown in Fig. 1(c), with $J/t=0.25$.

domain wall, and a zigzag domain-wall configuration becomes more likely than the diagonal configuration. In Fig. 3(c) we show the exchange field near a zigzag domain wall. Again, diagonal singlet correlations are present. In this case singlets are frustrating only near the ends of the wall.

So far we have characterized the states of the t - J model using the most probable hole configurations for typical systems. However, representing a system by a single hole configuration suggests that the holes are nearly static, which for small or moderate values of J/t is very far from the truth. A complementary viewpoint is obtained by studying “typical” hole configurations, chosen randomly from the probability distribution $\langle P(l_1, l_2, \dots) \rangle$. In Fig. 4(a) we show 12 typical configurations for a 14×4 system with 8 holes and $J/t=0.5$. These configurations were generated using a classical Monte Carlo algorithm to wander randomly through hole-configuration space, with acceptance probabilities $\langle P' \rangle / \langle P \rangle$ calculated at each Monte Carlo step using DMRG. The first configuration in the upper left is the initial, most probable one, showing two diagonal domain walls. Moving downward, successive configurations are separated by 240 Monte Carlo steps, enough to make them nearly uncorrelated. We see that in most of the configurations, there are no recognizable domain walls. From these configurations the holes appear to make up a strongly correlated gas, made up of clusters of two, four, and sometimes three holes. It is not obvious that the wave function represented by these configurations should exhibit the charge-density wave (CDW) structure expected from a set of domain walls.

In Fig. 4(b) we show the total average hole density per

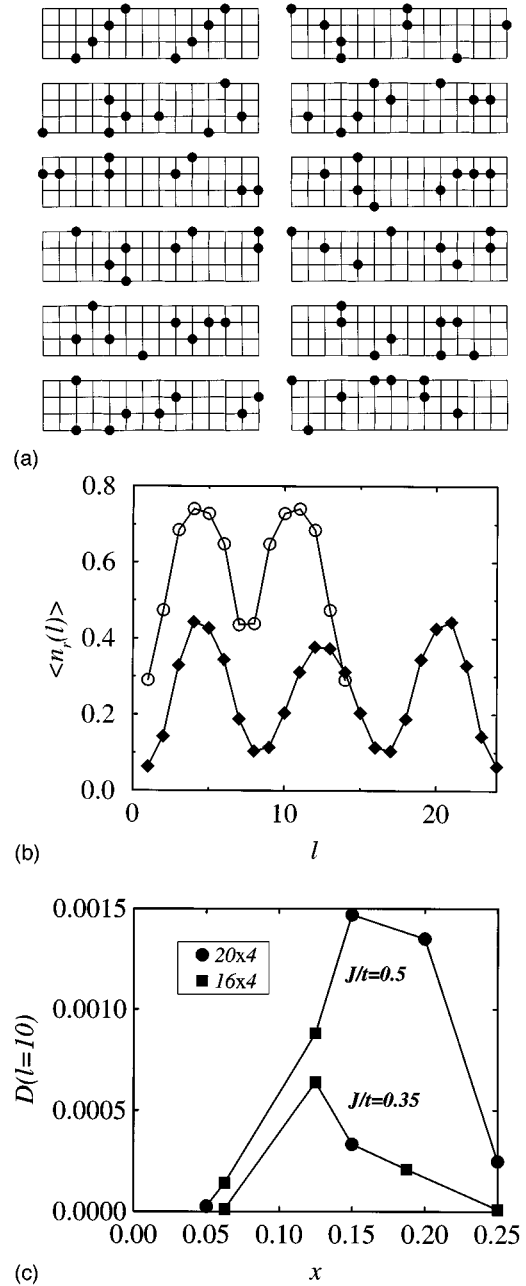


FIG. 4. (a) Typical hole configurations of a 14×4 lattice with $J/t=0.5$, and 8 holes. (b) The total average hole density on a rung as a function of the rung location. The upper curve is for the system shown in (a). The lower curve is for a 24×4 system with $J/t=0.35$ and 6 holes. (c) The equal time $d_{x^2-y^2}$ pair-field correlation function $D(l)$ at a separation of $l=10$ rungs versus doping x , for 20×4 and 16×4 systems and $J/t=0.35$ and 0.5 . The number of holes in each of the systems shown is a multiple of four.

rung $n_r(l)$ for the system shown in Fig. 4(a). We see that a strong CDW density variation is present, as one would expect from the maximum probability domain-wall pictures: the domain walls take up four rungs, and are separated by two rungs, which form a low-energy undoped two-leg ladder. These CDW domain-wall structures are subtle correlations built into the ground-state wave function, and are difficult to see in a limited number of hole-configuration snapshots, as in Fig. 4(a). The lattice sizes and dopings

shown have been chosen to match and enhance commensurate density variations, in which there are pronounced two-rung low-doping regions separating hole-rich domain-wall regions. It is not clear from the results we have so far whether there is commensurate long-range CDW order at special fillings (such as $x=1/6$), or a simple power-law decay of CDW correlations. We have not been able to study long enough lattices to characterize the behavior at incommensurate fillings: the system tends to adjust the filling at the two ends in order to lock up at a commensurate filling in the center. Also shown in Fig. 4(b) are results for a 24×4 system with $J/t=0.35$ and 6 holes, showing CDW correlations. In this case there are three separate pairs which give rise to these “ $4k_F$ ” CDW correlations, as opposed to the two-pair (four-hole) domain-wall structures of Fig. 1(b).¹¹ This behavior in the pair-gas state is similar to the pairing-CDW correlations observed in two-chain ladders.¹²

In Fig. 4(c) we show results for the equal-time $d_{x^2-y^2}$ pair-field correlation function, $D(l) = \langle \Delta_d(i) \Delta_d^\dagger(i+l) \rangle$, where $\Delta_d(i)$ destroys a nearest-neighbor $d_{x^2-y^2}$ pair at site i .⁹ The figure shows¹³ $D(l=10)$ as a function of doping x , with i_x and i_x+l_x chosen symmetrically about the center of the lattice, and with $i_y=i_y+l_y=2$. This quantity is useful as a measure of the overall strength of the pairing correlations. The pairing correlations for $J/t=0.5$ initially rise with doping, reaching a maximum between $x=0.15$ and $x=0.20$, and then decrease. Extended s -wave pairing correlations (not shown) are much smaller in magnitude. For $J/t=0.5$ the magnitude of the correlations near the maximum is similar to that seen in a two-leg Hubbard ladder with $U=8t$ (corresponding to $J \sim 4t^2/U=0.5$).¹² For $J/t=0.35$ the peak is reduced in magnitude and occurs at somewhat reduced doping. For $J/t=0.25$ the correlations (not shown) are less than 10^{-4} . The behavior of $D(l)$ versus l near the maximum (not shown) is consistent with a power-law behavior. Remark-

ably, the pairing correlations are larger in the domain-wall states than in the pair-gas states. The domain-wall states appear to exhibit “supersolid” behavior, with simultaneous pairing and CDW correlations. From the hole-configuration snapshots, we see how this can happen: the domain walls appear as an unbound resonance of hole pairs. There are also weaker resonances involving three-hole structures. These resonances are not strong enough to significantly weaken the pairing, and, in fact, the increased density of pairs in the domain-wall state leads to an increase in the pairing correlations relative to the more dilute pair-gas state, as seen in Fig. 4(c).

The domain-wall states we have found resemble in some respects the singlet striped phase proposed by Tsunetsugu, *et al.*¹⁴ In addition, various Hartree-Fock calculations,^{15–18} as well as Gutzwiller variational Monte Carlo calculations¹⁹ have found evidence for the formation of domain walls in the two-dimensional Hubbard model. The possibility that a CDW domain-wall state occurs prior to phase separation was suggested by Prelovsek and Zotos⁷ based on studies of four-hole correlation functions on small t - J clusters. Our present calculations show that domain-wall CDW ground states can occur in four-leg t - J ladders. The domain walls should be thought of as highly fluctuating resonances of pairs. These CDW domain-wall states have significant $d_{x^2-y^2}$ pair-field correlations, which are substantially stronger than in the low-doping pair gas.

We would like to thank S.A. Kivelson and T.M. Rice for useful discussions. S.R.W. acknowledges support from the NSF under Grant No. DMR-9509945, and D.J.S. acknowledges support from the Department of Energy under Grant No. DE-FG03-85ER45197, and from the Program on Correlated Electrons at the Center for Material Science at Los Alamos National Laboratory.

¹K. Kojima *et al.*, Phys. Rev. Lett. **74**, 2812 (1995).

²B. Batlogg *et al.*, Bull. Am. Phys. Soc. **40**, 327 (1995).

³M. Uehara, T. Nagata, J. Akimitsu, H. Takahashi, N. Mori, and K. Kinoshita, J. Phys. Soc. Jpn. **65**, 2764 (1996).

⁴S. R. White, Phys. Rev. Lett. **69**, 2863 (1992); Phys. Rev. B **48**, 10 345 (1993).

⁵S. R. White, Phys. Rev. Lett. **77**, 3633 (1997).

⁶For large values of J/t , DMRG can become stuck in metastable hole-cluster configurations, such as all in a cluster at one end rather than split into two clusters at the ends. To find the lowest energy state, one can initialize the DMRG iterations with the holes forced into specific locations, allow convergence, and then choose the calculation with the lowest final energy.

⁷P. Prelovsek and X. Zotos, Phys. Rev. B **47**, 5984 (1993).

⁸D. Poilblanc, Phys. Rev. B **49**, 1477 (1994).

⁹S. R. White and D. J. Scalapino, Phys. Rev. B **55**, 6504 (1997).

¹⁰An undoped two-leg ladder has a spin gap of order $0.5J$, which is associated with both a rise in the spin excitations and a lowering of the “vacuum” ground-state energy of the two-leg ladder

(Ref. 14). Thus an undoped two-leg ladder is a low-energy configuration.

¹¹Note that for the four-hole domain-wall state, the wavelength of the CDW structure is the length of the ladder L divided by one-fourth the number of holes ($4L/n_h=1/x$). For the dilute pair gas, this wavelength is L divided by one-half the number of holes, giving $2/x$.

¹²R. M. Noack, S. R. White, and D. J. Scalapino, Phys. Rev. Lett. **73**, 882 (1994).

¹³The amplitude of $D(l)$ is reduced by the square of the overlap of $\Delta_d(i)$ with a pair. For the simple near-neighbor operator we have used the overlap of order 0.1.

¹⁴H. Tsunetsugu, M. Troyer, and T. M. Rice, Phys. Rev. B **51**, 16 456 (1995).

¹⁵H. J. Schulz, J. Phys. (France) **50**, 2833 (1989).

¹⁶D. Poilblanc and T. M. Rice, Phys. Rev. B **39**, 9749 (1989).

¹⁷J. Zaanen and O. Gunnarsson, Phys. Rev. B **40**, 7391 (1989).

¹⁸J. A. Verges *et al.*, Phys. Rev. B **43**, 6099 (1991).

¹⁹T. Gimarchi and C. Lhuillier, Phys. Rev. B **42**, 10 641 (1990).